



## **CoastVal:**

# **Refactored Code Report**

### **TechWorks Marine Limited**

Pottery Road Enterprise Zone

Dun Laoghaire

Co. Dublin, Ireland



**CoastVal:**  
**Refactored Code Report**

Ref: ESA contract 4000118361

Date: 29/01/2021

Page: **2/26**

## 1. Contents

1. Contents.....	3
1. Introduction .....	5
2. System Setup .....	6
2. Data Processing.....	8
3. In Situ Data Processing Algorithm .....	9
4. In Situ Data Code .....	12
5. Biofouling.....	14
6. Satellite Data Processing .....	16
7. Results.....	18
8. Conclusion.....	18

**Date and Revision number:**

Reporting Date – 29/01/2021

Revision 1.0

This document has been prepared by:

Document					
Revision No.	Description	Prepared By	Checked By	Approved By	Issue Date
1		JL			
2					

**Signatory Legend:**

COK: Charlotte O'Kelly

Managing Director

SMcG: Sinéad McGlynn

Earth Observation Manager

JL: John Lavelle

Earth Observation Data Scientist

## 1. Introduction

This report describes the conversion of the CoastVal MATLAB code to Python and the analysis of the data. CoastVal is a validation platform for validating Sentinel-3 OLCI data. For more detail on the deployment, see “CoastVal Updated Deployment Report (July 2019)”.

The original code to process the data for this deployment was created by Karl Moore, the optical scientist working for TechWorks Marine at the time of the deployment. The code to process the data from the instruments on CoastVal was written in MATLAB, and SNAP was used for processing the satellite data. Processing the data was time consuming as it involved manual steps. The MATLAB code was rewritten in Python to make it easier to handle and extend and to automate the entire processing of both the in situ and satellite data. This allows bulk processing, enabling, for example, the validation to be quickly re-run for reprocessed OLCI data. This document describes the steps involved in processing the data.

**Commented [SM1]:** Needs standard cover page and layout of TechWorks documents

## 2. System Setup

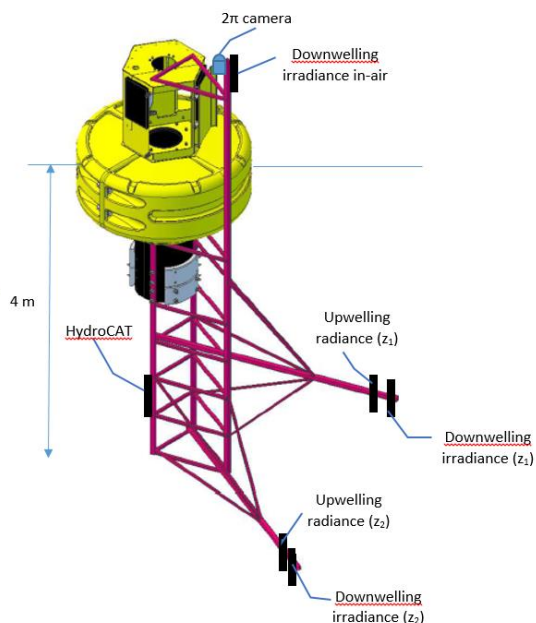


Figure 1: CoastVal buoy platform with sensor support structure.

The CoastVal hardware was identical to that used for the previous deployment in August 2018. The Mobilis DB2000 (see Figure 1) was fitted with a vertical support structure that extends 3.5 m below the water surface. From this scaffold support structure two arms extend horizontally 2 meters into the water column beyond the buoy perimeter. These arms are positioned at 2 and 3.5 m depth and offset 40° from each other to reduce shadowing effects and obstruction of the optical sensors. The buoy platform is approximately 1.9 m diameter and extends 1.35 m below and 1.5 m above the water surface.

A pair of upwelling radiance and downwelling irradiance sensors (Sea-bird Scientific HyperOCR) are attached to the end of each arm. The support frame ensures that a fixed depth separation is maintained between these sensor pairs and that all sensors maintain their viewing direction with respect to one another. The in-air downwelling irradiance sensor is attached to the top of the vertical boom structure. Each in-water sensor has a biowiper to reduce biofouling, which covers the sensor surface when the sensor is not operating.

Other sensors to measure conductivity, temperature, depth, and pH level (HydroCAT) and temperature and pressure (Seabird 39) were also added to the buoy platform, which were not included in the test deployment.

The support frame is fabricated from aluminium with the vertical boom and horizontal arms made with 50 x 50 mm square tubing. The vertical boom is constructed as part of a triangular structure with smaller 30 x 30 square tubing struts. The underside of the buoy and the support structure are painted black or covered with black tape to reduce any radiometric interference of the underwater light field. The precision depth sensor (Seabird 39 with pressure sensor option) is attached to the end of the lower sensor support arm with its transducer positioned (horizontally) between the up- and downwelling sensors.

The buoy platform is powered by solar panels and rechargeable batteries. To ensure optimal telemetry transmission for the duration of the deployment, 2 GSM antennas were added to the system.

**Commented [SM2]:** Font colour needs to be same as rest of the document

**Commented [JL3R2]:**

## 2. Data Processing

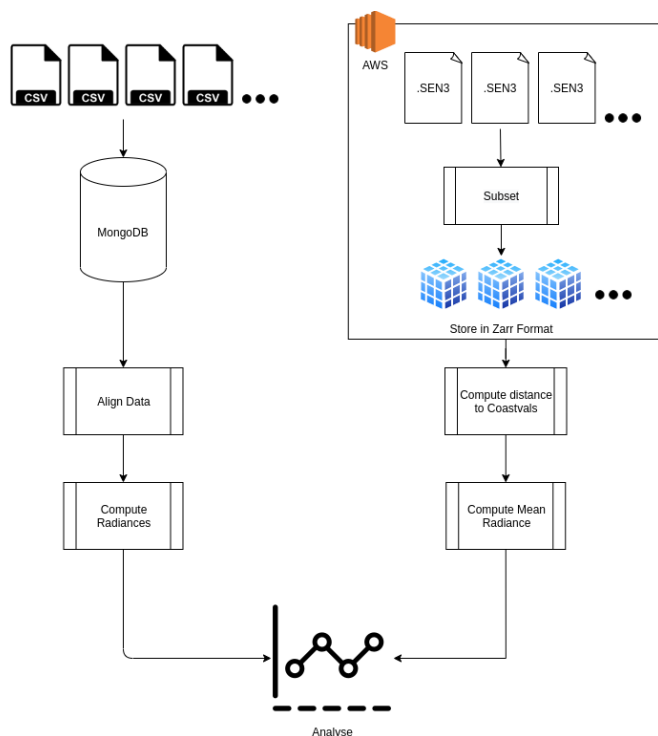


Figure 2: Processing steps for the processing of the CoastVal (see Section 3.1) and the satellite data (see Section 3.2)

Figure 2 shows an overview of the processing steps. The left side shows the processing steps for CoastVal and the right for the OLCI data. CoastVal collects data continuously for several hours each day. The data acquired at the time of the overpass is used in the validation. The data is stored in binary CSV files, containing the roll, pitch, heading from the IMU, water temperature, water pressure, the four spectral measurements. The data in the CSV files are unaligned. The CSV files from the deployment are inserted into a MongoDB database to make querying and aligning of the data easier. The CoastVal and OLCI data are processed and compared using a Jupyter Notebook. The code can be accessed on GitHub at [https://github.com/techworksmarine/coastval\\_data\\_analysis](https://github.com/techworksmarine/coastval_data_analysis).

**Commented [SM4]:** Please explain these steps in a bit more detail – what is contained within the CSV files? How much of the data acquired is used in the validation? Does it depend on S/N? The code can be accessed, but a non expert needs an overview of what it does.



### 3. In Situ Data Processing Algorithm

Several optical properties and parameters have been calculated in addition to the water-leaving radiance  $L_w$ , remote sensing reflectance  $R_{rs}$ , and water-leaving radiance reflectance or referred to here as simply 'reflectance'  $\rho_w$ . The remote sensing reflectance,  $R_{rs}$ , is related to the water leaving radiance,  $L_w$ , and the water-leaving radiance reflectance or directional reflectance,  $\rho_w$  by the simple relationships as shown below:

$$R_{rs}(\lambda) = \frac{L_w(\lambda)}{E_d^{0+}(\lambda)} \quad (1)$$

$$\rho_w(\lambda, \theta, \varphi) = \pi \frac{L_w(\lambda, \theta, \varphi)}{E_d^{0+}(\lambda)} \quad (5)$$

where  $E_d^{0+}$  is the downwelling irradiance measured in air and  $L_w$  is the water-leaving radiance just above the water in the upward direction measured by the satellite sensors whose observation position is defined by the zenith angle  $\theta$  and azimuth  $\varphi$ , that is,  $L_w(\lambda, \theta, \varphi)$ . These two equations have been presented in Equation (1) in the Measurement and Processing Algorithm document (March 2018).

The water-leaving radiance is given by,

$$L_{wn} = \frac{T_F}{n_w^2} L_{un}(0-), \quad (6)$$

where  $T_F$  is the Fresnel transmittance of radiance from water to air and  $n_w$  is the refractive index of water (generally assumed to be 1.34) and the upwelling nadir radiance by,<sup>1</sup>

$$L_{un}(0-) = L_{un}(z_1) \exp[K_{Lu} z_1] \quad (7)$$

where  $L_{un}(z_1)$  is the upwelling radiance measured at depth  $z_1$ , and  $K_{Lu}$ , the diffuse attenuation coefficient (a measure of how light dissipates with depth in water) for upwelling radiance is given by

$$K_{Lu} = \frac{1}{z_1 - z_2} \ln \left[ \frac{L_{un}(z_1)}{L_{un}(z_2)} \right], \quad (8)$$

where  $L_{un}(z_1)$  and  $L_{un}(z_2)$  are measured simultaneously by the two radiance sensors positioned at different depths.

<sup>1</sup> From MERIS Optical Measurements Protocol Issue 2, 2011, equation 32, pg. 74.

Or,

$$L_{wn} = \frac{T_F}{n_w^2} L_{un}(z_1) \exp\{K_{Lu} \cdot z_1\} \quad (9)$$

From equation (6) it can be seen that the uncertainty in the determination of the nadir water leaving radiance is dependent on the uncertainty in the upwelling radiance measurements at two depths, as well as the uncertainty in the measurements of those depths. It is also dependent on the value of,  $\frac{T_F}{\eta_w^2}$ , which (with  $n_w = 1.34$  and  $T_F = 0.97$ ) has a value of 0.543 (to within 1% under most conditions)

Note: The water-leaving radiance given above as  $L_{wn}$  has not been normalised to approximate the Sun at zenith or does it assume a mean Sun-Earth as does Sentinel Level 2 processing.  $L_{wn}$  here is the water-leaving radiance as viewed from nadir.

Although the satellite views the ocean at an oblique angle, its detection of water-leaving radiance is corrected to a nadir viewing position.

The uncertainty of  $L_w$  measured by CoastVal is dependent on a number of factors, including:

**1. Extrapolation Uncertainty**

Uncertainty in the determination of  $L_w$  due to extrapolation from the two upwelling radiance sensors at  $z_1$  and  $z_2$  to the surface

**2. Transmission through air-sea interface**

Fresnel transmission through air-water boundary ( $T_F$ ) is dependent on the sea state, i.e. wave height, wave/swell, direction (bidirectional effects), etc.. However, the uncertainty in  $T_F = 0.543$  has been determined to be much less than 1% for wind speeds up to  $20 \text{ ms}^{-1}$ .<sup>2</sup>

**3. Sensor depth**

Dependent on accuracy of pressure sensor and accuracy of mean depth for given wave height and integration time (averaging period).

**4. Sensor separation**

With sensors on extended booms there may be some flexing due to underwater currents, tidal flows etc. so that there might be some uncertainty.

**5. Tilt effects**

Nadir upwelling radiance at two depths, i.e.,  $L_{un}(z_1)$  and  $L_{un}(z_2)$ . Data can be filtered to utilise only tilt angles within  $\pm 5^\circ$ .

**6. Bottom reflectance**

The depth of the deployment site (ARB4) is roughly 32 m or approximately 28 m below the lowest (deepest) radiance sensor. To fulfil the requirement of 6 optical depths, the uncertainty can range between being negligible to 6% for attenuation coefficients ranging between 1 and  $0.1 \text{ m}^{-1}$ .

**7. Instrument accuracy: Radiance sensor**

- a. Stray light
- b. Radiometric calibration (wavelength allocation and spectral response)

<sup>2</sup> Voss, KJ and S. Flora 2017. "Spectral Dependence of the Seawater-Air Radiance Transmission Coefficient." *J. Atmos. Ocean. Technol.*, 1203-5.

8. **Biofouling:** downward-facing sensors are less prone to biofouling of the fore-optics and at depth

Also the uncertainty in  $E_d^{0+}$  is dependent on the in-air sensor:

1. **Tilt effects:** Pitch and roll (if less than 5° in pitch or roll then error  $\sim < 0.38\%$  in terms of the irradiance sensor and if pitch and roll are both  $\sim 5^\circ$  then error is approximately  $< 0.54\%$  due to cosine response alone). This does not include error of the cosine collector from true cosine response.  
“The impact of tilt may be particularly strong in sunny (satellite validation) conditions because of the highly anisotropic light field. Its impact on the measurement uncertainty can be estimated if two angles of tilt with respect to the sun and approximate angular variation of sky radiance are known.”<sup>3</sup>
2. **Instrument accuracy: Irradiance sensor**
  - a. Stray light
  - b. Solar zenith angle and angular response of irradiance cosine collectors
  - c. Radiometric calibration (wavelength allocation and spectral response).
3. **Biofouling:** effects of sea spray, atmospheric deposition of particles, rain droplets, insects etc. These can only be monitored by frequent calibration checks such as by the use of relative calibration devices.

In order to more accurately compare the water leaving radiance measured by CoastVal and OLCI, the Spectral Response Function of the OLCI instrument should be taken into account. Figure 3 shows the spectral response function of each of the Sentinel-3 bands.

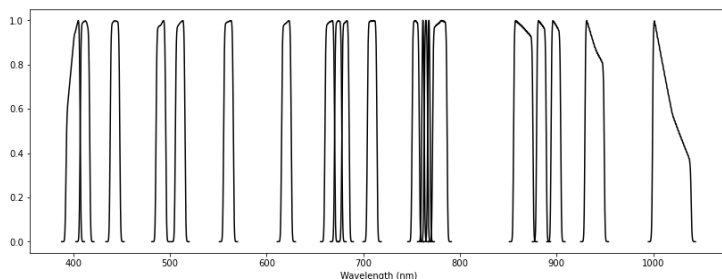


Figure 3: The spectral response functions of Sentinel-3/OLCI.

<sup>3</sup> FRM4SOC TR-1, section 3.1.2.1

**Commented [SM5]:** Actually I don't know if all of these were included in the most up to date code Karl ran, please check and see which are incorporated into your modified python code.

**Commented [JL6R5]:** These are the causes of uncertainty. It is true that they are not used to estimate the uncertainty but it is still good to state the causes of uncertainty

The water leaving radiance which is measured by OLCI,  $R_b$ , for band, is given by

$$R_b = \int_{-\infty}^{+\infty} R_{rs}(\lambda) \text{SRF}_b(\lambda) \delta y,$$

where  $\text{SRF}_b(\lambda)$  is the Spectral Response function for the given band,  $b$ .  $\text{SRF}_b(\lambda)$  is available from <https://sentinel.esa.int/web/sentinel/technical-guides/sentinel-3-olci/olci-instrument/spectral-response-function-data>.  $R_{rs}(\lambda)$  and  $\text{SRF}_b(\lambda)$  are measurement at for discrete values of  $\lambda$ ; therefore  $\text{SRF}_b(\lambda)$  is interpolated and resampled to wavelengths for which CoastVal is measured. Simpson's rule is then used to do the integration.

## 4. In Situ Data Code

This data is stored in binary files. The data covers the period 2019-07-09 to 2019-10-13 and is comprised of 3,498 files, totalling 2.7 GB. The first step in the processing chain is to transfer the data from the binary files to a MongoDB database. MongoDB is a NoSQL database and is used to enable querying of the data.

MongoDB should be installed on the system and run with the following command:

```
mongod
```

The program is run with the following command:

```
python3 preprocess_insitu/coast_val_to_mongodb.py data/2019/
```

where data/2019/ contains the CSVs (in binary format).

The next step, shown in Figure 3, is to align the data. The radiances, inclinometer and temperature data are inserted in three corresponding collections (tables) in MongoDB. For each radiance measurement, the maximum roll and pitch is computed and inserted in another table.

The next step is to compute the radiances, with the following command:

```
python3 coastval_data_analysis/coastval_spectrum.py
```

The generates a HDF5 file contains all the compute spectra. The steps involved in computing these spectra are explained in Section **Error! Reference source not found.**

The algorithm is implemented in the following code snippet from coastval\_spectrum.py:

```
data = {instrument: datas for instrument, datas in get_data(start, end)}
df = reindex_dataframe(data)

# Compute the radiances & irradiances, with the arguments given in radiance_dict.
# The radiance is computed for each spectra in the timeseries in the dataframes.
spectra = {rad_name: radiance(df, instrument1, instrument2)
            for rad_name, (instrument1, instrument2) in radiance_dict.items()}
# spectra = pd.concat(spectra, axis=1)
# Load the Sentinel-3 Spectral Response Functions
```

```

wavelengths_centre_exact = data_sent_srf['SRFF'].flatten()
wavelengths_centre = np.round(wavelengths_centre_exact, 2).astype(np.float16)
# Spectral response interpolation-function dictionary for each band
msrf_dict = {i + 1: interp_msrf(i) for i in range(data_sent_srf['MSRFwavelength'].shape[1])}

# Compute the radiance/irradiances. Get a dictionary of timeseries of these spectra
spec_s3bands = {spec_name: spectra_measured_by_sentinel3(spectra[spec_name], wavelengths_centre,
msrf_dict)
                for spec_name in radiance_dict.keys()}

# Compute the upwelling radiance just below surface
dz1 = 2
KLus = (np.abs(np.log(spec_s3bands['tradiance_w1'] / spec_s3bands['tradiance_w2'])) / 1.475)
KLu = KLus.mean(axis=0)
Lun0minus = spec_s3bands['tradiance_w1'] * np.exp(KLu * dz1)

# Compute the water-leaving radiance
etaw = 1.34 # calculated refractive index for input salinity and temperature for each wavelength
Tf = 0.97 # Fresnel reflectance will be different and must be calculated
# for lower solar elevation angles. That is, for SEA ~45 Tf = ~0.96, or fpr
# SEA ~30 deg. Tf = 0.93
Tws = Tf / etaw ** 2
Lwn = Tws * Lun0minus

# Remote sensing reflectance
Rrs = (Lwn / spec_s3bands['tirradiance_a']) * np.pi

```

## 5. Biofouling

CoastVal was affected by biofouling during the deployment [2]. Spectra that were affected by biofouling need to be identified in order to be excluded from the validation. The instrument was manually cleaned on the 18<sup>th</sup> of September.

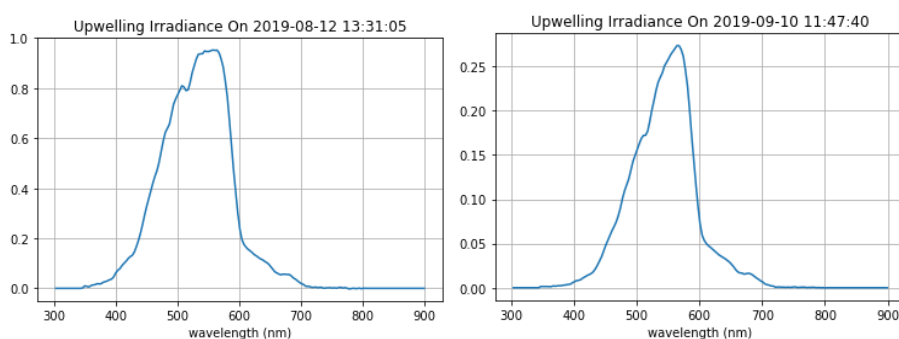


Figure 4: The figure on the left shows the downwelling irradiance where the sensor is not affected by biofouling and the figure on the right is an example where the measurement is degraded due to biofouling.

There are 21,527 sets of spectral measurements during the deployment. Figure 4 shows examples of irradiance measurements with and without biofouling issues. The biofouling reduces the amplitude of the spectrum and reduces, with a greater reduction at lower wavelengths. Non-Negative Matrix Factorization (NMF) is used to decompose the spectra into two components. In NMF a matrix,  $S$ , is given by

$$S = WH,$$

where  $W$  and  $H$  are the weight and bases matrices respectively and  $S$  is the matrix with the reconstructed spectra. This method is used because it can be easier to interpret than methods whose components are not restricted to positive numbers, such as Principal Component Analysis (PCA).

Figure 5 shows the components given by the NMF. These components explain 83% of the variance in the spectra. The first and second components appear to well characterise the spectra affected by biofouling spectra shown in Figure 4. Figure 6 shows the weights of these components as a function of time. During the beginning of September, the weight of the first component increases, while the second decreases, indicating biofouling. The ratio of the first component to the second is plotted in Figure 7. A high ratio of From Figure 7, the biofouling issue appears to have begun around August 30<sup>th</sup> until it was cleaned on the 18<sup>th</sup> of September.

Commented [SM7]: Unfinished sentence

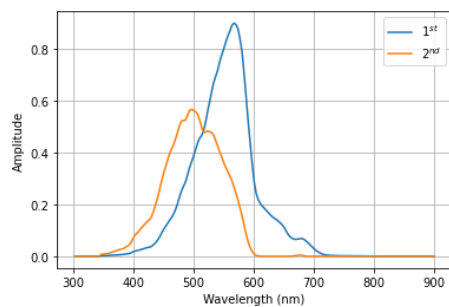


Figure 5: The components of the irradiance.

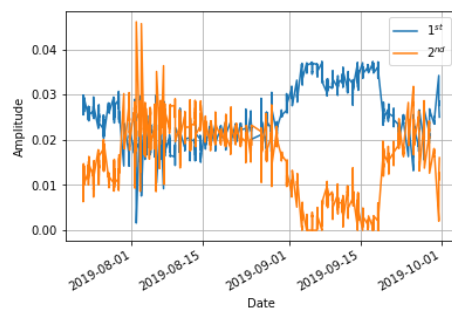


Figure 6: The weighting of the first and second components.

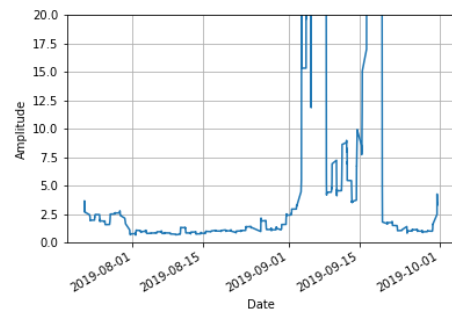


Figure 7: The ratio of the first to the second components.

## 6. Satellite Data Processing

CoastVal was deployed on the 30<sup>th</sup> of July 2019. During that time, 11 Sentinel-3 overpasses were acquired for which CoastVal was collecting data (see Appendix 2). The quality of the data was affected by biofouling for some dates and (see Appendix 2). See Section 3 for a description of the method used to detect biofouling.

Figure 2 shows the Sentinel-3 processing steps. The CoastVal measurements were validated against the satellite measurements following [1]. This document recommends a spatial window of 3×3 pixels for non-homogenous conditions. The first step is to select read the pixels close to CoastVal that are to be used from the validation.

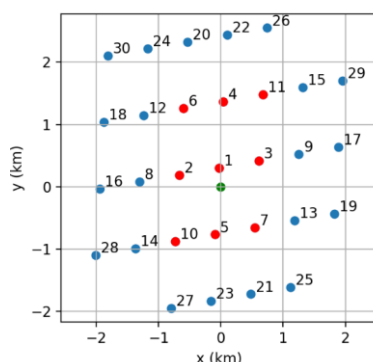


Figure 8: The location of CoastVal and the centre of the Sentinel-3 pixels nearby to CoastVal.

Figure 8 shows the location of CoastVal relative to the Sentinel-3/OLCI pixels. The green dot indicates the location of CoastVal. The red and blue pixels show the location of the Sentinel-3 pixels relative to CoastVal, numbered in order of distance to CoastVal, with one being the closest. The 3×3 pixels closest to pixels, shown in red, are selected for the validation. These nine pixels are necessarily the closest; in this case, the 8<sup>th</sup> and 9<sup>th</sup> pixels are not included. For each band, the mean spectra of the nine pixels is calculated.

The following code is run to compute the nearest neighbours. The first step is to subset the OLCI product files with

```
preprocess_sentinel3/subset_s3.py
```

This program saves the data close to CoastVal in the Zarr format. The next step is to compute the nearest neighbours, as described above, with:

**Commented [SM8]:** This needs more detail, mean of what? Which pixels?



`preprocess_sentinel3/compute_nearest_neighbours.py`.

## 7. Results

The satellite and in situ data are compared in the following Jupyter notebook:

```
compare_spectra.ipynb
```

The MongoDB database should be running for this notebook to work.

The results of the analysis are shown in Appendix 2. There are eleven simultaneous CoastVal and OLCI measurements, for which there was least partially clear skies. Biofouling affected four of these acquisitions and cannot be used for validation purposes. There are four acquisitions with clear skies and no biofouling; these are indicated with a ✓ to the right of the plot; there are the acquisitions on 2019/08/02, 2019/08/08, 2019/08/23 and 2019/09/20.

For the acquisition on 2019/08/02, the reflectances are consistently lower for across all the OLCI bands, relative to CoastVal. For OLCI band 11 (708.75 nm) the reflectivity is negative (an invalid value). The CoastVal acquisitions have a high variance, possibly due to sea waves.

The OLCI acquisition on 2019/08/08 is a very good match between CoastVal and there is low variance in the CoastVal measurements. There OLCI reflectances are slightly higher than CoastVal below 510 nm and slightly lower above 510 nm, for most bands.

For the acquisition on 2019/08/23, there is a fairly good match between the two, particularly above 510 nm. There is a high variance in the CoastVal measurements below 510 nm, which may explain the poorer match at the lower wavelengths. The cause of the higher variance in the CoastVal measurements at the wavelengths is unknown.

For the acquisition on 2019/09/20, there is a poor match between the two spectra, except for the higher and lower wavelength bands. The reason for the mismatch is unknown.

## 8. Conclusion

There are four acquisition which could be used for validation purposes, another seven acquisition were rejected due to the biofouling CoastVal or clouds. Two of the four OLCI acquisitions had a good match with the Sentinel-3, while the other two had a relatively poor match. It is difficult to express this in more quantitatively due to the low number of samples.

Further work could be done on following the validation protocols more closely (see [1]). For example, the protocol recommends filtering out outlier pixel value from the nine pixels in the vicinity of CoastVal. Also, the time window over which the CoastVal spectra are average may not be optimal. The data has been stored in a single NetCDF file (with the CoastVal and OLCI data aligned) making further analysis convenient.

Reposessed OLCI data, provided by EUMETSAT, is used in the analysis described here. In a future analysis, atmospheric algorithms in SNAP, for example C2RCC, could be applied to the OLCI Level-1 data to compute the reflectivity. C2RCC allows parameters such as salinity and temperature to be provided. Salinity and temperature was measured during the deployment, but was not used in this analysis, and could be used to improve the accuracy of the computed OLCI reflectivity.









The data processing pipeline demonstrated here could be applied to online processing in a future validation project. At the time of writing TWM is converting moving it's computing resources to AWS. AWS. Data from the in situ measurement could be stored on AWS' Dynamodb. Dynamodb could be used in place of Mongoddb, used here, as it is similar. The rest of the code could be adapted and automatically run when a new satellite acquisition is obtained.

## Appendix 1



































The both the CoastVal and OLCI data is saved as a NetCDF file. The following is a Xarray of description of the file:

► Dimensions: (band: 16, time: 12, times: 260)

▼ Coordinates:

<b>times</b>	(times)	datetime64[ns]	2019-08-02T10:47:31.290000 ... 2...		
<b>band</b>	(band)	object	400.2 411.8 443.0 ... 768.0 779.5		
<b>time</b>	(time)	datetime64[ns]	2019-08-02T10:47:28.063948 ... 2...		
wavelength	(band)	float64	400.3 411.8 ... 884.3 1.016e+03		

▼ Data variables:

altitude	(time)	float32	dask.array<chunksize=(1,), meta=np.nda...		
chl_nn	(time)	float32	dask.array<chunksize=(1,), meta=np.nda...		
chl_oc4me	(time)	float32	dask.array<chunksize=(1,), meta=np.nda...		
iop_nn	(time)	float32	dask.array<chunksize=(1,), meta=np.nda...		
mask	(time)	float64	dask.array<chunksize=(1,), meta=np.nda...		
reflectivity	(time, band)	float32	dask.array<chunksize=(1, 1), meta=np.n...		
reflectivity_err	(time, band)	float32	dask.array<chunksize=(1, 1), meta=np.n...		
reflectivity_satpy	(time, band)	float32	dask.array<chunksize=(1, 1), meta=np.n...		
satellite_azimut...	(time)	float64	dask.array<chunksize=(1,), meta=np.nda...		
satellite_zenith_...	(time)	float64	dask.array<chunksize=(1,), meta=np.nda...		
solar_azimuth_...	(time)	float64	dask.array<chunksize=(1,), meta=np.nda...		
solar_zenith_an...	(time)	float64	dask.array<chunksize=(1,), meta=np.nda...		
trsp	(time)	float32	dask.array<chunksize=(1,), meta=np.nda...		
tsm_nn	(time)	float32	dask.array<chunksize=(1,), meta=np.nda...		
wqsf	(time)	float64	dask.array<chunksize=(1,), meta=np.nda...		
Rrs	(time, times, band)	float64	0.01168 0.01283 ... 6.893e-05		
Rrs_mean	(time, band)	float64	0.01227 0.01334 ... 5.042e-05		

The variable “reflectivity” is the OLCI reflectivity, where the OLCI pixels have been averaged as described in Section 3. The variable “reflectivity\_err” is the uncertainty from the OLCI product. The variable “Rrs” are the CoastVal is the reflectivity measurements measured during the OLCI acquisition. The “Rrs\_mean” is “Rrs”, averaged with respect to time.

The data is aligned with respect to time, so, for example, the difference between the CoastVal and OLCI reflectivities can be given by:

```
(ds['Rrs_mean'] - ds['reflectivity_satpy']).dropna(dim='time')
```

using Xarray, where ds is the dataset.

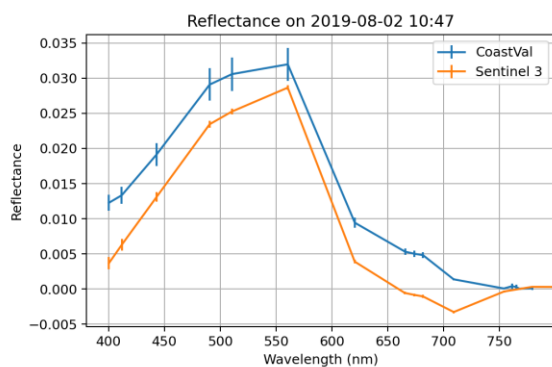
## Appendix 2

The CoastVal and OLCI data have been plotted together here, to allow direct comparison.

The name of the OLCI product is given under the plot. The prefixes S3A and S3B indicate the particular Sentinel-3 satellite. The OLCI product was reprocessed on 2020/10/27.

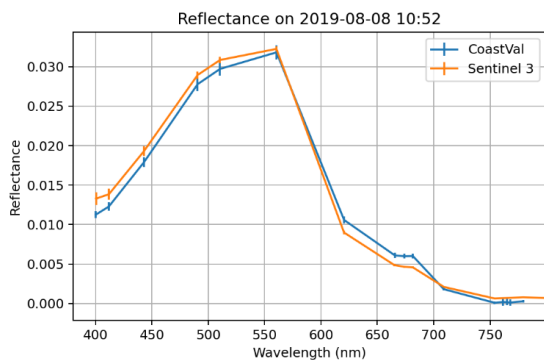
There error bars for CoastVal are given by the standard deviation of the spectral measurements within the time window. The error bars for Sentinel-3 is the uncertainty of the product.

Comments are given on the right column. ✓ indicates that the measurements is considered suitable for analysis and X indicates that the measurements are excluded for use for validation due to clouds or biofouling.



S3A\_OL\_2\_WFR\_\_20190802T104728\_20190802T105028  
20201027T132738\_0179\_047\_322\_0000\_MAR\_O\_NT\_002

Low biofouling  
Clear Skys  
High CoastVal Error  
Negative OLCI values  
✓

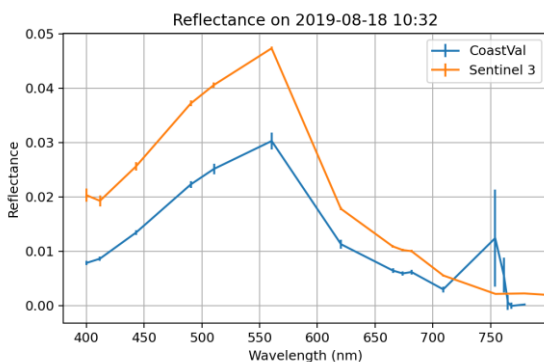


Low biofouling

Clear Skys

✓

S3B\_OL\_2\_WFR\_\_\_\_20190808T105248\_20190808T105548  
 \_20201027T132751\_0179\_028\_265\_0000\_MAR\_R\_NT\_002

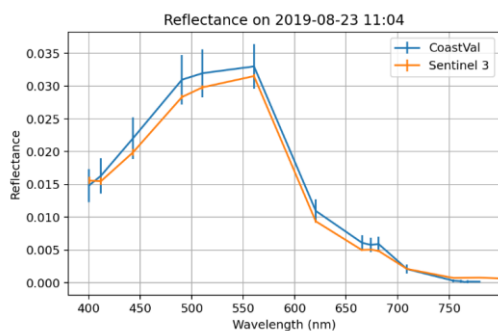


Low biofouling

Relatively clear but  
cloud

X

S3A\_OL\_2\_WFR\_\_\_\_20190818T103228\_20190818T103528  
 \_20201027T132742\_0180\_048\_165\_0000\_MAR\_O\_NT\_002

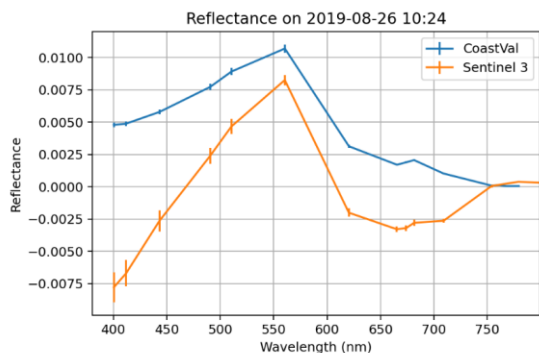


Low biofouling

Scattered but clear shot

✓

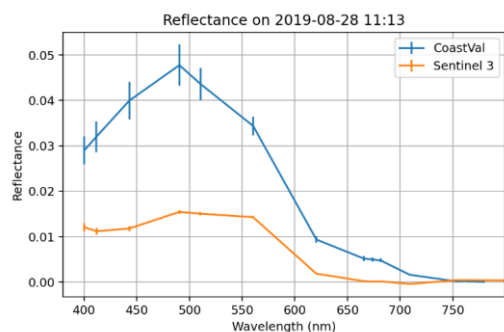
S3B\_OL\_2\_WFR\_\_\_\_20190823T110401\_20190823T110701  
 \_20201027T132741\_0179\_029\_094\_0000\_MAR\_R\_NT\_002



Low biofouling  
 Clear but cloud effects  
 Negative OLCI values

X

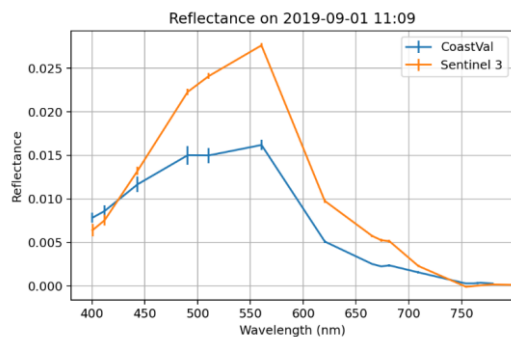
S3A\_OL\_2\_WFR\_\_\_\_20190826T102458\_20190826T102758  
 \_20201027T132735\_0179\_048\_279\_0000\_MAR\_O\_NT\_002



Low biofouling

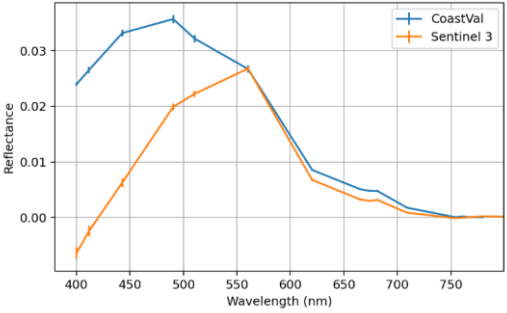
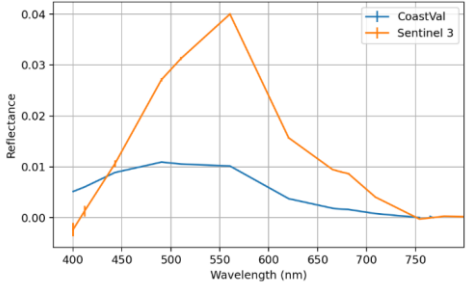
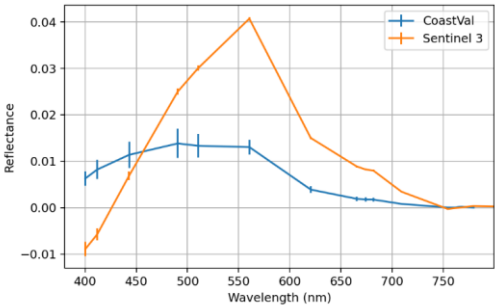
X

S3A\_OL\_2\_WFR\_\_\_\_20190828T111335\_20190828T111635  
 \_20201027T132739\_0180\_048\_308\_0000\_MAR\_O\_NT\_002

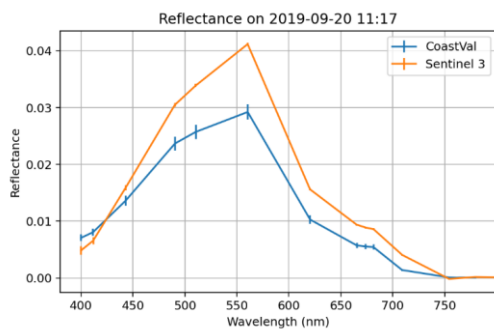


Possible Biofouling

X

S3A_OL_2_WFR____20190901T110951_20190901T111251 _20201027T132734_0179_048_365_0000_MAR_O_NT_002	
<p>Reflectance on 2019-09-10 10:36</p>  <p>S3A_OL_2_WFR____20190910T103613_20190910T103913          _20201027T132734_0179_049_108_0000_MAR_O_NT_002</p>	<p>Possible Biofouling</p> <p>X</p>
<p>Reflectance on 2019-09-17 10:54</p>  <p>S3A_OL_2_WFR____20190917T105456_20190917T105756          _20201027T132734_0180_049_208_0000_MAR_O_NT_002</p>	<p>Possible Biofouling</p> <p>X</p>
<p>Reflectance on 2019-09-18 10:28</p>  <p>S3A_OL_2_WFR____20190918T102845_20190918T103145          _20201027T132739_0179_049_222_0000_MAR_O_NT_002</p>	<p>Possible Biofouling</p> <p>X</p>





S3A\_OL\_2\_WFR\_\_\_\_20190920T111722\_20190920T112022  
 \_20201027T132746\_0180\_049\_251\_0000\_MAR\_O\_NT\_002

Low biofouling

Very clear



## Bibliography

1 Recommendations for Sentinel-3 OLCI Ocean Colour product validations in comparison with in situ measurements – Matchup Protocols

2 CoastVal Updated Validation Report, Karl Moore, 2019-10-09